Are we really targeting and stimulating DLPFC by placing tES electrodes over F3/F4?

Ghazaleh Soleimani[1], Rayus Kuplicki[2], Jazmin Camchong[1], Alexander Opitz[3], Martin P Paulus[2], Kelvin O Lim[1], Hamed Ekhtiari[1,2*]

[1] Department of Psychiatry, University of Minnesota, MN, USA

[2] Laureate Institute for Brain Research (LIBR), OK, USA

[3] Department of Biomedical Engineering, University of Minnesota, MN, USA

#Corresponding Author:
Hamed Ekhtiari, MD, PhD
Department of Psychiatry, University of Minnesota,
M Health Fairview University of Minnesota Medical Center – West Bank
606 24th Ave S, Minneapolis, MN, 55454, USA

Highlights

- In most frequently used DLPFC tES montages, EF peaks were not located under the electrodes
- The EF peak in DLPFC montages is located in the medial frontopolar area
- An independent clinical population showed slight between-group differences
- There is a large interindividual variation in both location and strength of the EF peak

Abstract (283 words)

Background: Most transcranial electrical stimulation (tES) clinical trials place target electrodes over DLPFC based on the assumption that it would mainly stimulate the underlying brain region. Here, we assessed delivered electric fields (EF) using a symmetric and asymmetric DLPFC stimulation montage to identify additional prefrontal regions that are inadvertently targeted beyond DLPFC.

Methods: Head models were generated from the human connectome project database's T1+T2-weighted MRIs of 80 healthy adults. Two common DLPFC montages (symmetric: F4/F3, asymmetric: F4/Fp1 with 5×7cm electrodes, 2mA intensity) were simulated. Averaged EF was extracted from (1) the center of the target electrode (F4), and (2) the top 1% of voxels that showed the strongest EF in individualized EF maps. Inter-individual variabilities were quantified with standard deviation (SD) of EF peak location and value. These steps were replicated with 66 participants with methamphetamine use disorder (MUD) as an independent clinical population.

Results: In the healthy adults, EFs in the frontopolar area were significantly higher than EF "under" the target electrode in both symmetric (peak:0.41±0.06, F4:0.22±0.04) and asymmetric (peak:0.38±0.04, F4:0.2±0.04) montages (Heges'g>0.7). Group-level location for EF peaks in MNI space was located in the medial-frontopolar cortex, such that individualized EF peaks were placed in a cube with a volume of symmetric/asymmetric: 29cm^3/46cm^3. Similar results (with slight between-group differences) were found for MUDs that highlighted the role of the medial frontopolar cortex in both healthy and clinical populations.

Conclusions: We highlighted that in common DLPFC tES montages, DLPFC was not maximally targeted and the frontopolar area was the area that received the highest EFs. Considering inter-individual and inter-groups variability, we specifically recommended that the frontopolar role should be considered as a potential mechanism underlying the clinical efficacy of DLPFC stimulation.

Keywords: Transcranial electrical stimulation, transcranial direct current stimulation (tDCS), bipolar montage, dorsolateral prefrontal cortex (DLPFC), frontopolar cortex, computational head models, electric field (EF).

1. Introduction

The dorsolateral prefrontal cortex (DLPFC) is important for many neurocognitive processes [1, 2]. Impairment of neuroplasticity in the DLPFC has also been reported in different neuropsychiatric diseases such as depression [3], schizophrenia [4], and substance use disorders (SUDs) [5]. In this regard, DLPFC is commonly used in non-invasive brain stimulation methods including transcranial magnetic (TMS) or electrical (tES) stimulation as a promising intervention target [6, 7].

Recent advancements in TMS coil placement (e.g., neuro-navigation systems [8] or fMRI-informed target selection [9]) provide optimized and individualized approaches for DLPFC targeting [10]. However, in tES studies, the 10-20 standard system is widely used for targeting and placing the electrodes over DLPFC [11]. This system proposes an appropriate method to link the external scalp locations to the underlying cortex which is typically used in electroencephalography (EEG) electrode placement [12]. With respect to the previous meta-analyses, in tES protocols, stimulating electrodes are typically placed over the F4/F3 locations to modulate the right/left DLPFC [13]. It has been shown that F4/F3 coordinates over the scalp correspond with DLPFC locations in the cortex [14]. Most clinical trials place stimulation electrodes over the scalp based on the assumption that the target electrode (e.g., over F4/F3) will mainly stimulate the underlying brain region (e.g., DLPFC) as the main target. However, using gyri-precise head models, it has been shown that tES electrodes produce diffuse current flow and maximal electric fields (EFs), corresponding to areas of maximal stimulation, can fall outside the target electrodes rather than underneath them as commonly assumed [15-17].

Despite the diffusivity of the current [18], the effects of placing electrodes over F4/F3 have been attributed to modulation of the right/left DLPFC even in recent publications [19, 20] and less attention has been paid to the possibility that a strong EF in other regions can contribute to the observed clinical/behavioral outcomes of DLPFC-targeting protocols. EF modeling and delineation of different cortical regions (e.g., by defining spheres around a specific coordinate or using atlas-based parcellation), may help provide a useful quantitative comparison of the electrical dose delivered to different targeted or non-targeted brain areas. Based on the analysis of both normal and tangential components of the EFs in modulating prefrontal cortex, Csifcsak et al reported that strong stimulation can be found not only in DLPFC but also in the medial prefrontal cortex (MPFC) in bipolar montages which are commonly used for depression [21]. Their study supported previous modeling studies that have suggested the medial prefrontal cortex as a new target for depression in TMS studies [22, 23]. In another example of atlas-based parcellation of the computational head models, four different electrode arrangements were simulated for a single standard subject (ICBME152) and 22 cortical areas were extracted per hemisphere [22]. That study demonstrated that maximum values of tangential and normal components of EFs were located in the orbital and frontopolar cortices when using an F3-Fp2 montage [24].

Previous works pointed out the importance of inter-individual variability of the EF and submaximal stimulation dose at the intended target [25], suggesting the need for a systematic analysis of dosage in targeted and non-targeted regions. EF variation has been linked to substantial differences in morphological features (e.g., skull thickness, cortex morphology, and gyrification [26, 27]). These differences may explain why cortical EF is not restricted to a region “under” the electrode; understanding the distribution of the peak current density and its cortical location in a large sample may help to design more optimal protocols and better interpret stimulation outcomes at both individual and group-levels.

In this context, the primary goal of this study is to evaluate the site/strength of the maximum tES-induced EFs in the prefrontal cortex at a group-level while considering two of the most used electrode montages for DLPFC stimulation (anode/cathode over F4/F3 and F4/Fp1) with 2 mA stimulation intensity in both clinical and healthy populations. This work highlights the importance of considering tES-induced EFs on brain regions that are not located underneath the stimulating electrodes and support a model-driven approach for tES target determination.

2. Materials and Method

2.1. Participants

Unprocessed T1 and T2-weighted structural MRIs from 80 (44 female) randomly selected healthy adults (age (year) between 31-35 (n = 32, 15 female), between 26-30 (n = 34, 21 female), between 22-25 (n = 14, 8 female) (the exact age of participants are not reported in the database) were obtained from the freely available Human Connectome Project database (HCP, http://www.humanconnectomeproject.org/data/) with deidentified anatomical scans. Structural MRI data in the HCP data archive were collected with a Siemens MAGNETOM 3T scanner with 32 channel head coil and the following parameters for T1-weighted MRIs: TR/TE = 2400/2.14, flip angle = 8, the field of view = 224 x 224 x 180 mm3 and voxel size = 0.7 mm3, and T2-weighted MRIs: TR/TE = 3200/565. More details on imaging parameters and data acquisition can be found in the HCP database, Appendix I: Structural Session Scan Protocol.

2.2. Creation of head models and EF simulations

Individualized computational head models were generated from a combination of high-resolution T1 and T2-weighted MRIs. Head models were created for all 80 subjects using the standard SimNIBS 3.2 pipeline [28]. Briefly, T1 and T2-weighted images were segmented into six tissue types, including white matter (WM), gray matter (GM), cerebrospinal fluid (CSF), skull, scalp, and eyeballs, using an automated tissue segmentation approach in SPM 12 based on the “headreco” function. Segmentation results were evaluated carefully slice by slice to ensure proper tissue classification. Tetrahedral volume meshes with about 3×106 elements were created for each head model and visualized using Gmsh and MATLAB. Three subjects were removed due to problems with the head generation process. Gmsh failed to mesh one or more surfaces in 3 attempts for two subjects. In another subject, mesh generation failed in decoupling between white matter and gray matter ventricles. All results were reported based on EFs for 77 healthy subjects.

Two of the most commonly used conventional tES montages for targeting DLPFC were simulated for all subjects by placing 5×7 cm electrodes with 1 mm thickness over (1) F4/F3 (symmetric montage) and (2) F4/Fp1 (asymmetric montage). A standard EEG cap (EEG10-10-UI-Jurak-2007) was used for placing electrodes over the scalp. In the symmetric montage, centers of the target electrodes were located over F4 and F3 locations with the long axis of the pads pointing towards the vertex of the head. In the asymmetric montage, the forehead electrode (Fp1) was positioned over the left eyebrow with the long axis of the pad parallel to the horizontal plane (as shown in Figure 1, panel b). Here we focused on 35 cm^2 rectangular electrodes since this size/shape was by far the most commonly used in previously published studies (e.g., in our updated systematic review in the field of addiction medicine, among total of 67 published studies, only 4 studies used circular while 38 studies used two 5x7 electrode [29]). However, the orientation of non-circular electrodes can affect the strength and direction (normal component) of

the EFs over the cortex. Therefore, the locations and orientations of the electrodes were precisely checked in Gmsh to guarantee consistency after automatic placement using a modified MATLAB code in SimNIBS.

Through the SimNIBS pipeline, the finite element method (FEM) was used to simulate EFs for head meshes. Linear and isotropic electrical conductivities were assumed based on previously established conductivity values for each tissue type [17]: white matter = 0.126, gray matter = 0.275, cerebrospinal fluid = 1.654, skull = 0.010, skin = 0.465, and eyeballs = 0.5 all in Siemens per meter (S/m). The absolute and normal components of the EFs were calculated for each montage and each individual. Surface-based head models were then transformed from individualized space to the "fsaverage" standard space (http://surfer.nmr.mgh.harvard.edu) to make the results comparable across the population in terms of brain coordinates. Although normalization to the standard space can affect EF distribution patterns, our previous study showed no statistically significant difference between the group-level results obtained from standard space and subject space [25].

2.3. Data analysis methods

Averaged EF strength was extracted from the main regions of interest (ROIs) in the prefrontal cortex (please see 2.4) for each individual. Peak EF was defined as the 99th percentile of the EF over the cortex and both location and strength of the peak were extracted at the individual and group levels. Between-subject variations were quantified using the relative standard deviation (SD) of the EFs strength and locations. Numerical statistical analyses were performed using the *R* package. As the Shapiro-Wilk test of normality showed our database is normally distributed, t-tests were used to examine significant differences between EFs in two separate brain regions. All data reported as mean ± SD. Statistical results were reported based on P values and Hedges' g factors to explain the level of significance and effect sizes.

2.4. Defining regions of interest (ROI)

In order to compare EF strength over DLPFC and around peaks, two individualized 10 mm spheres were defined: (1) around the center of the target electrode (F4) location, and (2) around 99th percentile of the EFs for each individual. Spheres were combined with the MNI mask to ensure analyses did not include EFs from non-brain or white matter voxels.

The Brainnetome atlas (which has a fine-grained parcellation of the cortex as a multimodal parcellation atlas based on structural MRI, diffusion tensor imaging, and resting-state fMRI connectivity) was used for the parcellation of the computational head models [30]. Inspired by [31], ROIs were placed in 9 main subregions in the Brainnetome atlas; Superior frontal gyrus: A9l, lateral area [13,48,40], A9m, medial area [6,38,35], A10m: medial area [8,58,13]. Middle frontal gyrus: A9/46d, dorsal area [30,37,36], A9/46v, ventral area [42,44,14], A46 [28,55,17], A10l, lateral area [25,61,-4], and Orbital gyrus: A11l, lateral area [23,36,-18], A11m, medial area [6,57,-16]. Averaged EF strength was calculated for each of the 9 prefrontal subregions. Differences between subregions were calculated using ANOVA and posthoc pairwise t-test.

2.5. Replication of the results with a sample of the clinical population

Based on our updated systematic review on transcranial electrical stimulation trials (tES) in substance use disorders (SUDs), by May 2022, 66 out of 75 tES electrode montages (88%) in SUDs with successful outcomes in modulating drug craving and drug consumption used bipolar DLPFC stimulation with symmetric or asymmetric montages [29]. However, less attention has been paid to the distribution of tES-induced EFs in the field of addiction medicine. In order to determine the replicability of the results in a

clinical population, all previous steps were repeated for 66 participants (age (year) between 18-60, all male) with methamphetamine use disorders (MUDs) as a representative example of a clinical population (more details about participants, T1 and T2 MRIs, and data collection protocols can be found in our previously published paper [25]).

3. Results

3.1. Comparing EFs in the center of target electrodes and hot spots

Individual and group-level analysis of personalized head models showed that the 99th percentile of the EFs (peaks) is not located underneath the stimulating electrodes (F4; [40.5, 41.4, 27] coordinate over the cortex in MNI space). Averaged locations for the peak EFs across the population were [-1.21, 57.66, 18.67] for symmetric and [-2.62, 49.00, -4.54] for asymmetric montages (please see section 3.3 for more details on inter-individual variations in terms of locations and EF values). With respect to the brain anatomical subregions, EF peaks were located within the frontopolar area; a region occupying the anterior portion of the brain's frontal lobe (dominantly corresponding to Brodmann's area 10) which is distinct from DLPFC (which is located on the lateral and dorsal part of the medial convexity of the frontal lobe [32]) where the stimulating electrode was placed (dominantly comprises Brodmann's areas 9 and 46) [2]. In both electrode montages, averaged EFs in a 10 mm sphere around the peak EFs (symmetric: 0.32±0.07, asymmetric: 0.24±0.05; mean ± SD in V/m) was significantly (P value for: symmetric = 3.01x10^-4, asymmetric: 4.52x10^-6) higher than a 10 mm sphere around F4 location over the cortex in which the center of the target electrode was placed (symmetric: 0.22±0.05, asymmetric: 0.19±0.05 in V/m) with large effect sizes (Hedges'g for: symmetric = 0.8598 with 95% CI (0.53,1.19) and asymmetric = 0.7630 with 95% CI (0.43,1.09)). Our results also showed that, in both locations, underneath the electrode and averaged peaks the symmetric montage produced significantly (P = 0.00015) higher EFs compared to asymmetric electrode arrangement with medium effect sizes (Hedges'g for: symmetric = 0.6234 with 95% CI (0.95, 0.30) and asymmetric = 0.7965 with 95% CI (0.47, 1.13)).

As shown in Figure 1, EFs were also extracted in the coordinates related to the individualized 99th percentile and center of the stimulating electrode (without averaging within 10 mm spheres) and similar results were found. EF strength in the coordinate related to the 99th percentile (symmetric = 0.41±0.06, asymmetric = 0.38±0.05) was significantly (P value = 2.2x10^-16 for both montages) higher than the coordinate related to the center of stimulating electrode (symmetric = 0.23±0.05, asymmetric = 0.20±0.04) with large effect sizes (Hedges'g for: symmetric = 3.2091 with 95% CI (2.73, 3.69) and asymmetric = 3.8339 with 95% CI (3.30, 4.37)). EFs were also significantly higher in the symmetric montage compared to asymmetric (P value for: 99th percentile = 0.004, the center of target electrode = 1.7x10^-5) with small effect sizes for 99th percentile individualized coordinate (Hedges'g = 0.4724 with 95% CI (0.15, 0.79)) and medium effect size for the coordinate related to the center of target electrode (Hedges'g = 0.7114 with 95% CI (0.34, 1.04)).

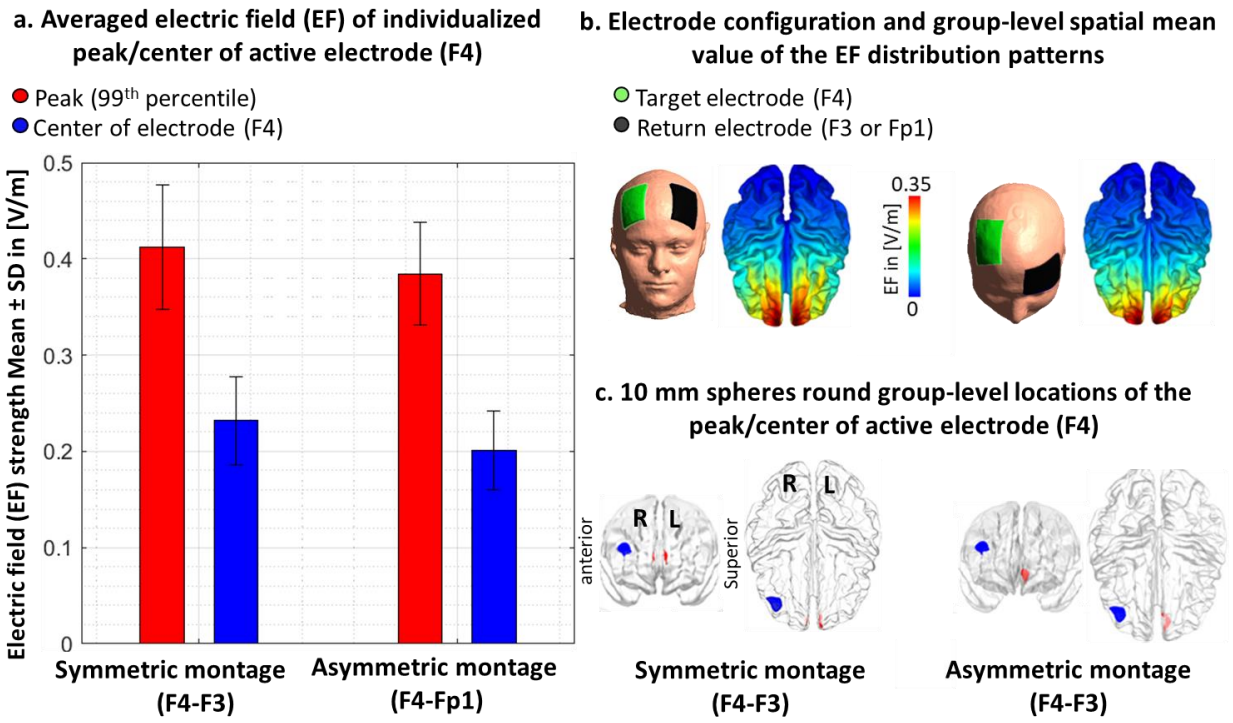

Figure 1. Comparing EF (electric field) in the center of the target electrode vs. peak EF. (a) Bars show mean values and error bars show standard deviations (SD) of the EF strength in volt per meter ([V/m]) across 77 healthy subjects in individualized 99th percentile of the EF (peak EF, in red) and center of the target electrode (F4, in blue) over the cortex across the population for symmetric (target/return electrodes over F4/F3 in dark colors) and asymmetric (target/return electrodes over F4/Fp1 in light colors) montages. **(b)** Electrode configurations over the scalp for DLPFC stimulation are visualized with the target (in green)/return (in black) electrodes over F4/F3 in symmetric and F4/Fp1 in asymmetric montages. EF distribution patterns at the group-level (spatial mean values across the population) are visualized over the cortex in superior view. **(c)** Locations of the 10 mm spheres around F4 (in blue) and averaged location of the peak EF across the population (in red) are visualized over the standard brain in fsaverage space. In each panel, the left side corresponds to the symmetric montage (F4-F3) and the right side corresponds to the asymmetric (F4-Fp1) montage.

3.2. Inter-individual variabilities

Inter-individual variability in terms of peaks' locations and strength was compared across the population. Variations across the population are visualized in Figure 2. In the symmetric DLPFC stimulation, the mean location for the peaks across the population in MNI space was [-1.21, 57.66, 18.67] with [6.43, 4.37, 8.08] as SD, and all peak locations were placed in a cube with a volume of 29 cm3 (X = 3.1, Y = 1.9, Z = 4.9). Group-level mean value for the EF strength was also 0.41±0.06 [V/m] (ranges from 0.31 to 0.68). In the asymmetric DLPFC stimulation, the mean location for the peaks in MNI space was [-2.62, 49.00, -4.54] with [7.05, 7.71, 8.94] as SD, and all peak locations were placed in a cube with a volume of 46 cm3 (X = 3.3, Y = 3.4, Z = 4.1). Group-level mean value for the EF strength was also 0.38±0.04 [V/m] (ranges from 0.28 to 0.59).

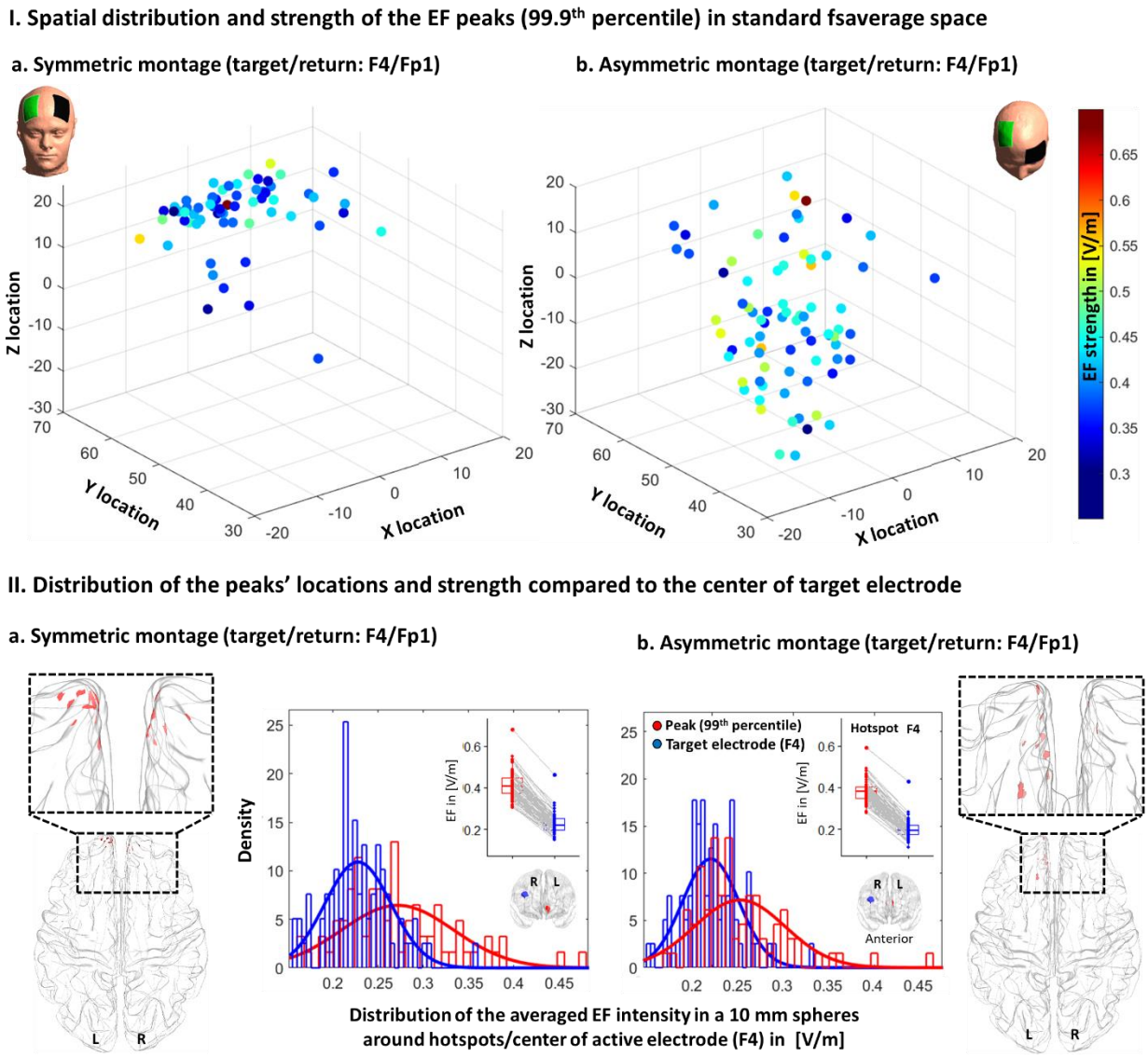

Figure 2. Inter-individual variability of electric field (EF) strength and locations. I. Scatter plot (for location in MNI space) colored based on EF strength (hot colors represent strong EF strength) for visualizing inter-individual variability in peaks (99th percentile) of the EFs in (a) symmetric and (b) asymmetric DLPFC montages. **II.** Visualizing the location of the 99th percentile of the EF over the standard fsaverage space (red dots over the cortex represent each individual). Distribution plots represent the distribution of the EF strength within the 10 mm spheres around F4 and 99th percentile (blue and red spheres over the cortex in anterior view) for (a) symmetric and (b) asymmetric montages. Boxplots showing differences between EFs in the coordinates related to individualized peaks and F4 in [V/m]. Dots and spaghetti lines over the boxplots represent the data for individual subjects. Abbreviation: EF: electric field.

3.3. Atlas-based parcellation results

In addition to the spherical ROIs around the center of target electrode (DLPFC) and peaks (medial frontopolar), averaged EFs were also extracted from the main regions of the prefrontal cortex including

superior frontal gyrus (SFG), middle frontal gyrus (MFG), and orbital gyrus (OrG) in the Brainnetome atlas (areas related to the Brodmann area 9, 10, 11, and 46 as defined in the method section); SFG: A9l, A9m, A10m, MFG: A9/46d, A9/46v, A46, A10l, OrG: A11m, and A11l. Averaged EFs in each subregion in both left and right hemispheres along with the representation of the regions over the cortex can be found in the supplementary materials (Figure S1). Cumulative EF strength with a symmetric montage in the right frontopolar (A10m + A10l) was significantly ($P<0.01$ with Hedges' $g = 0.3412$) higher than right DLPFC (A9/46v+A9/46d). Additionally, symmetric montage induced slightly higher EFs compared to the asymmetric montage in almost all subregions but differences were significant only in the A10m in both hemispheres ($P<0.001$).

3.4. Replication results in a clinical population

All above-mentioned steps were replicated for a group of participants with methamphetamine use disorder (MUD) as an independent clinical population. Similar to the healthy subjects, inter-individual variability was found in both location and strength of the EFs across the population. In the symmetric montage averaged location for the EF peaks in MNI space was [1.88, 60.34, 19.12] with [5.71, 3.34, 6.72] as SD, and all peaks were placed inside a cube with a volume of 21.7 cm^3. In the asymmetric montage averaged location of the EF peaks in MNI space was [-3.14, 56.90, 6.33] with [7.37, 5.86, 9.74] as SD, and all peaks were placed in a cube with a volume of 45.9 cm^3. Our EF strength results (Figure S2 in supplementary materials) showed that EF strength in the frontopolar area (symmetric: 0.31±0.07, asymmetric: 0.32±0.07) where EF peaks were placed is significantly ($P<0.001$) higher than DLPFC (symmetric: 0.18±0.05, asymmetric: 0.19±0.05) underneath the target electrode with large effect sizes (Hedges'g for symmetric = 1.6190 with 95% CI (1.19, 2.04) and asymmetric = 1.3599 with 95% CI (0.95, 1.77)). However, no significant difference ($P > 0.1$) was found between the EFs strength in symmetric and asymmetric montages in this population such that effect sizes were negligible (for peak EFs Hedges'g = 0.13 with 95% CI (-0.24, 0.50) and around F4 location Hedges'g = -0.02 with 95% CI (-0.39, 0.34)). Additionally, by considering inter-individual variability (Figure S3 in supplementary materials), in atlas-based parcellation of the head models, results (Figure S4 in supplementary materials) showed that the frontopolar area (A10l+A10m) received a significantly higher EF strength compared to DLPFC (A9/46v+A9/46d) in both symmetric and asymmetric montages ($P<0.001$).

Our results showed that averaged peak location in symmetric (healthy: [-1.21, 57. 66, 18.67], MUDs: [1.88, 60.34, 19.12] with maximum 4.12 mm^3 Euclidean distance from F4 location over the cortex) and asymmetric montages (healthy: [-2.62, 49, -4.54], MUDs: [-3.14, 56.9, 6.33] with maximum 13.45 mm^3 Euclidean distance from F4 location over the cortex) have a substantial overlap between the two groups such that in both groups peaks were located within the frontopolar area (Figure 3). Furthermore, using an unpaired t-test for between-group comparison in terms of EF strength in spherical regions around peaks, a significantly higher EF strength in the asymmetric montage in the MUD (0.31±0.07) was found compared to the healthy group (0.23±0.05) with a medium effect size (Hedges' $g = 0.6172$ with 95% CI (0.27,0.97)). A significant difference in the symmetric montage was also found around the F4 location with a higher EF strength in the healthy group (0.23±0.05) compared to MUDs (0.18±0.04) with a large effect size (Hedges' $g = -0.9059$ with 95% CI (-1.27,-0.55)).

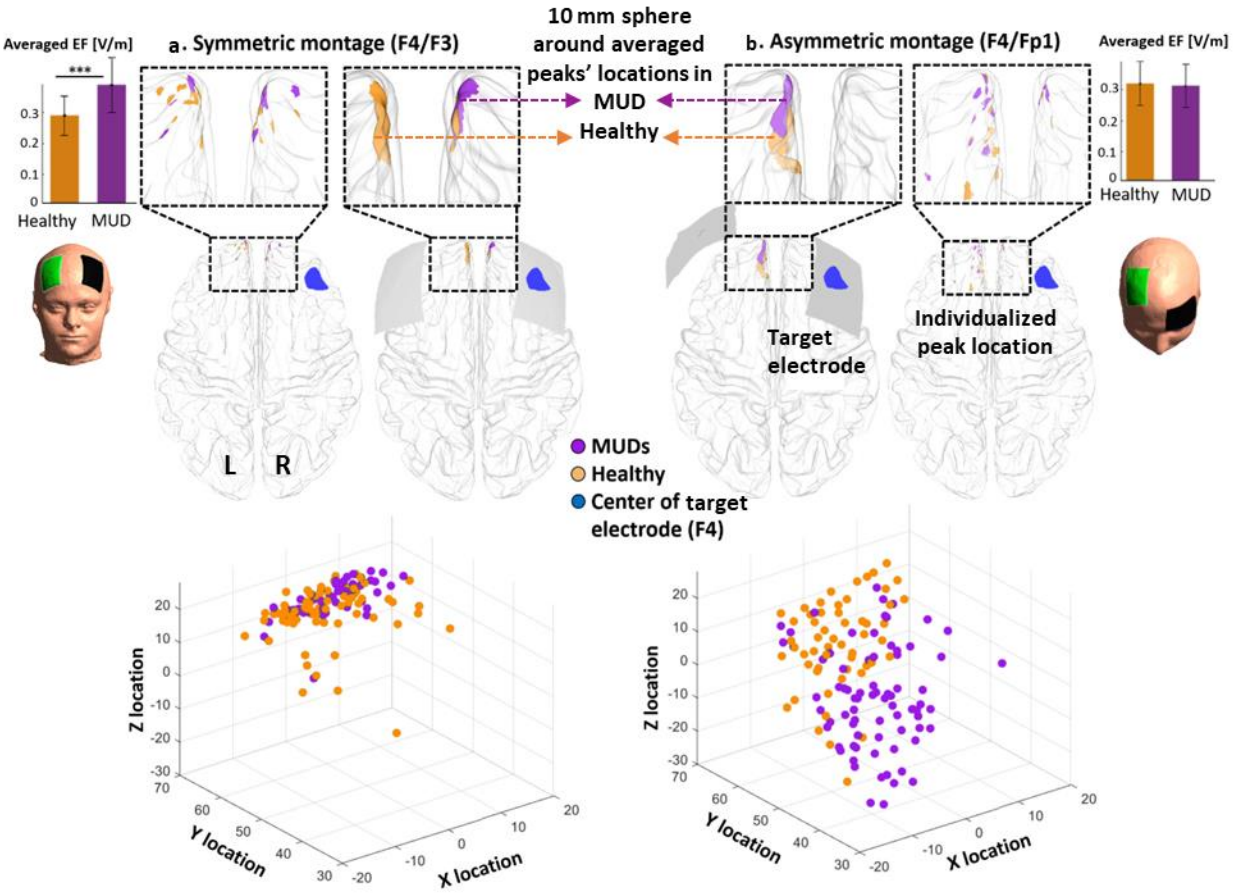

Figure 3. Comparison between healthy subjects and methamphetamine users in terms of location and strength of the peaks at both individual and group levels. Overlap between 10 mm spheres around mean EF peaks in healthy subjects (in brown) and a group of participants with methamphetamine use disorders (in purple) compared to the center of the target electrode F4 (in blue) in both symmetric (left panel) and asymmetric (right panel) montages. Small dots represent each individual in each group and big circles represent 10 mm spheres around averaged peaks' locations at the group-level. MNI coordinates for F4 = [40.5, 41.4, 27], averaged peak location in the symmetric montage (F4/F3): healthy subjects = [-1.21, 57.66, 18.67] and methamphetamine users = [1.88, 60.34, 19.12] with 4.12 mm3 Euclidean distance, asymmetric montage (F4/Fp1): healthy subjects = [-2.62, 49, -4.54], methamphetamine users = [-3.14, 56.90, 6.32] with 13.45 mm3 Euclidean distance.

4. Discussion

In this study, we modeled the target selectivity of two of the most frequently used electrode montages for modulating DLPFC; symmetric (anode/cathode: F4/F3) and asymmetric (anode/cathode: F4/Fp1) montages to explore whether and to which extent DLPFC could be the main target compared to other brain regions that are not intentionally targeted but received strong electric field (EF). Individualized computational head models were generated for two groups of participants; healthy participants and people with methamphetamine use disorders (MUDs). Specifically, this investigation yielded four main results. First, the peaks of EF are located far (45.54 Euclidian distance in MNI space) from DLPFC (F4

location as the center of target electrode). Second, group-level EF peaks were dominantly placed near the medial frontopolar cortex in both montages and both healthy participants and people with methamphetamine use disorder (MUD) groups, such that peak EF (99th percentile) received significantly higher EFs compared to the cortical area under the center of the target electrodes; DLPFC. Third, variations were found within and between groups in terms of EF peaks' location and strength.

4.1. Importance of peak EFs in brain stimulation studies

Our computational approach with a substantial sample size underlies the utility of head models for uncovering potentially stimulated brain regions based on EF peaks. As investigated in previous brain stimulation studies [33], the efficacy of the stimulation protocol may vary depending on the brain region being modulated. However, systematic analysis of EF distribution patterns and finding the association between tES-induced EFs and stimulation outcomes requires a decision about which EF measures (e.g., maximum (99^{th} percentile to remove outliers), mean, median, or a binary thresholded EF map) are appropriate to use. Here, inspired by previously published studies in the field [34, 35], we focused on EF peaks to provide an indicator of the location at which the target activity is most likely to be perturbed [36]. Then, peak EF location and strength in the peak location were compared with the cortical area under the center of target electrodes as the main "intended" anatomical target.

In the application of tES with large electrode pads (conventional tES), it has been repeatedly reported that maximal EF is not underneath the electrodes but rather between them and outside the "area under the electrode" [15, 37, 38]. With respect to the diffuse current flow, it's not surprising that we found EF peaks out of DLPFC; similar to previous studies on motor cortex stimulation that reported maximum EFs between two electrodes [39]. However, our data suggest that top 1% of voxels with the highest EF is located farther from the intended cortical target (DLPFC). Therefore, if the main goal of the stimulation is reaching the brain area beneath the target electrode (F3/F4), it is recommended to define an ROI in the targeted brain region and extract averaged value from no-threshold EF maps.

4.2. Inter-individual variability

Our results showed significant inter-individual variability in the location and strength of the peak EF in directly/indirectly targeted brain areas which are in line with previous studies that emphasize the importance of considering personalized head models [26, 37, 38]. The main issue with the inter-individual variability of EFs over the cortex is that the potential effect of tES is limited by small effect sizes and it would be difficult to detect intervention effects at the group-level [40-42]. Different sources of variability including anatomical parameters (e.g., fat thickness, skull thickness, and amount of CSF that affect current flow through the brain) affect EF distribution patterns [26, 43-45]. The variability of the simulation results indicates that personalized electrode montages should be considered to have similar cortical stimulation doses inside a target area across a population.

4.3. Atlas-based vs spherical ROIs

Our atlas-based parcellation results further support the results obtained from ROI definition based on considering the peak and center of target electrode locations such that EF strength in the right frontopolar was higher than right DLPFC. Although the most common approach for exploratory ROI analysis (e.g., in fMRI analysis) is to create small spheres around the peaks' locations (e.g., peaks of activation clusters),

atlas-based parcellation may help to simply explore and localize informative regions (e.g., subregions of the prefrontal cortex involved in DLPFC stimulation) based on the spatial distribution patterns of the EFs. However, as suggested by [46], the specific brain parcellation of each atlas impacts the spatial accuracy of the extracted brain regions especially when differences in the observed EF distribution patterns are small. Hence, in accordance with recent research [47], the Brainnetome atlas, with fine-grained parcellation of the prefrontal cortex, was used to accurately extract how EF was distributed through the subregions of the prefrontal cortex. Nonetheless, regions specified with atlas-based parcellation could be large (e.g., entire SFG), and even if the region contains highly modulated nodes, strong EFs may only occur in a small proportion of vertices in the ROI. This suggests that by simply averaging across a parcel spatial detail about the EF will be lost. Focusing on individualized brain EF maps and defining ROIs based on personalized EF distribution patterns or using a fine-grained atlas (e.g., Schaefer atlas [48]) might be a better approach compared to averaging through a large parcellated brain area.

4.4. DLPFC montages make peak EF in frontopolar areas

There is converging evidence highlighting the role of brain regions with strong EFs like frontopolar as a novel stimulation target for non-invasive brain stimulation for designing new clinical trials [49-52]. In this context, our findings about strong stimulation strength within the frontopolar cortex in commonly used electrode montages over DLPFC are in line with a previous modeling study that reported strong EF intensity within the medial prefrontal cortex (MPFC) rather than DLPFC in all commonly used bipolar DLPFC electrode montages in depression [21]. This study suggested that symptom improvement in DLPFC tES trials in depression might not necessarily be specifically related to the DLPFC and other brain areas with strong EF (e.g, MPFC) may also contribute to the tES treatment outcomes. Furthermore, preliminary evidence from clinical trials confirmed associations between EF strength and behavioral changes in depression [31]. For instance, in a DLPFC stimulation study with electrodes over F5/F6 locations in a group of participants with major depressive disorder (MDD), a significant positive correlation between EFs within the MPFC-dorsal area (A9/46d) and behavioral outcomes was reported. While the correlation between EFs in DLPFC (A9 and A46) and the same behavioral outcome (negative affect) was negative (greater score reductions were associated with lower EF strength). Taken together, a brain region with higher EFs might be linked to behavioral outcomes through several psychophysiological mechanisms and neural substrates. Therefore, based on our simulations, we argue that conventional electrodes over DLPFC also stimulated the frontopolar area. We recommend taking into account the cognitive process associated with the frontopolar region in the interpretation of the results in conventional tES studies over DLPFC [26, 43-45].

4.5. Dose-response relationship

Here, we only focused on highly modulated brain regions with respect to the strong EF over the cortex using high-resolution structural MRI data. It has been assumed that brain regions with higher EFs contribute to greater alteration in brain responses and may have stronger effects on stimulation outcomes (e.g., higher EFs followed by greater functional alterations) [53]. Under the assumption that EF strength over the cortex relates to the tES responses at the functional level, the association between stimulation dose and brain responses in a cortical target could explain dose-response relationships in tES studies. Recent advancements in neuroimaging (like fMRI) and neurophysiology (like TMS) suggest a complicated non-linear and state-dependent dose-response relationship in tES studies. However, there are still some supporting evidence that highlight the role of brain regions with strong EFs in physiological/neural

response to tES that may help to determine the role of DLPFC and frontopolar area and the importance of brain regions with higher EFs in symmetric/asymmetric DLPFC stimulation studies.

One of the earliest studies in which both EFs and fMRI data were discussed was by Halko et al 2011. The single-subject case study of tDCS with combined visual rehabilitation training after stroke revealed that EF strength was correlated with task-based fMRI activation in some predefined ROIs; higher EF was linearly related to stronger functional activation [54]. In a group of participants with left-sided glioma, averaged EF strength was extracted from the left and right M1 ROIs, and a significant correlation between averaged EFs in the right M1 and changes in global resting-state connectivity from the right M1 was reported [55]. Antonenko et al. also assessed the relationship between tES-induced EFs and neurophysiological outcomes and significant negative/positive correlations were reported between the tangential/normal component of the EF and resting-state functional connectivity in the sensorimotor cortex [56]. Additionally, Jamil et al investigated whether cerebral blood flow (CBF) activations across the cortex agree respectively with EFs obtained from head models. Using a voxel-wise rank correlation, a significant correlation between averaged EF distribution patterns in MNI space and the group-level T-contrast images was reported at the voxel-level in both cathodal and anodal stimulation [57]. Recently it has also been shown that current density in the left DLPFC positively correlated with changes in functional connectivity between two predefined ROIs (left dorsolateral and left ventrolateral PFC) during a working memory task based on using psychophysiological interaction analysis and simulating precise computational head models [58]. All previous dose-response relationships highlight the importance of EF strength and its effects on stimulation outcomes that shed light on how modulated brain areas with stronger EFs may affect the response to stimulation. A similar investigation approach (which has not been investigated in healthy subjects) is needed to assess dose-response relationships in the frontopolar area while DLPFC is targeted. In addition to correlational methods, testing for the causal role of the frontopolar in DLPFC stimulation studies can help to confirm the importance of the frontopolar cortex in the regulation of stimulation outcomes.

4.6. Bipolar montages (asymmetric vs. symmetric) induce different EF patterns in the frontal lobe

Another finding in this study was significant differences between symmetric and asymmetric montages in terms of EF strength in healthy subjects. As we discussed in our previous publication with a network-based perspective [25], cathode location significantly affects EFs strength in targeted or non-targeted brain areas [38, 59]. Here, we found that symmetric DLPFC stimulation induced significantly higher EFs in both DLPFC and peaks compared to asymmetric montage. Lower EF strength in asymmetric montages could be related to a lower distance between the electrodes over the scalp compared to the symmetric montage [60]. It can be attributed to more current shunting in asymmetric montage compared to symmetric since electrodes are in closer proximity [61]. More significant changes in behavioral outcomes using symmetric DLPFC stimulation might be related to the stronger cortical EFs compared to asymmetric montages. For instance, previous studies showed that symmetric montages over DLPFC could diminish risk-taking behavior during a Balloon Analogue Risk Task (BART) [62, 63], while asymmetric DLPFC stimulation shows no such effect [64]. Between montage difference in terms of peaks' strength only in the healthy group (not MUDs) suggest that generalization of the results obtained from EF distribution patterns fundamentally depends on the population of interest and highlights the importance of head modeling in tES protocol optimization in both individual and group levels [65, 66].

4.7. Optimized tES targeting: Converging evidence from HD-tES, neuroimaging, and TMS studies

In this study, we only focused on conventional large electrode pads and electrode positioning based on EEG standard system because clinical tES typically uses conventional electrodes and scalp-based landmarks to target the DLPFC. Conforming with previous computational head modeling studies, our results revealed that placing stimulating electrodes directly above the cortical target does not guarantee its optimal stimulation dose under the electrode. More focal electrode montages could help to focus on the stimulation target. With respect to the previous systematic reviews [67], there is a lack of evidence for using focal stimulations over the predefined ROI using precisely targeted high-definition (HD) montages for the treatment of neuropsychiatric disorders [67]. In order to modulate DLPFC as the main target, instead of large pads, HD electrodes could be placed over this brain region to be focally stimulated. Our results suggested that in commonly used montages for targeting DLPFC, DLPFC did not receive the highest EF intensity. An optimization algorithm could be used to find an electrode montage to maximally target DLPFC while minimizing EF in non-targeted brain areas. With HD electrodes/optimized montage placed over DLPFC, the frontopolar area could receive much less stimulation. If desired, the frontopolar region could be stimulated using a separate set of HD electrodes. However, its efficiency and tolerability (by fixing small electrodes over the forehead) should be further assessed in experimental trials [11].

Additionally, fMRI-informed montage selection is a promising step towards more efficient and precise brain stimulation protocols which has recently started to gain momentum, especially in the field of TMS [68-70], and potentially provides valuable information about functional localization to guide EF peak locations based on modulating active neural circuits or functional networks [71, 72]. Closing the loop between brain-state and stimulation parameters may also help to increase the efficiency of the optimization algorithm using concurrent tES-fMRI. In this context, stimulation dose (e.g., current strength, electrode location, frequency, and phase difference) could be optimized at an individual level to maximally stimulate the ongoing brain state [73].

4.8. Considering network-based modulation

Using atlas-based parcellation of the head models, we argued that placing the electrodes over DLPFC modulated multiple nodes in the prefrontal cortex which has the potential to act synergistically to enhance stimulation outcomes through excitatory/inhibitory pathways between two anatomically distinct brain regions. It has been reported that the contribution of brain regions in response to tES-induced EFs through brain networks would be more effective than modulating a single network node [74]. In this regard, the distribution of the EFs and peaks' location could be optimized based on the interaction between main network nodes. Previous tES-fMRI studies suggest that network-based electrode montages led to a better outcome compared to conventional stimulation montages [72]. However, there is subtle nuance in the application of tES with a network-based approach especially with conventional electrodes [75]. Considering HD or multi-array electrodes may be more efficient for network-based targeting.

4.9. Substance use disorders as a sample clinical population

Here, we considered a group of participants with MUDs as an independent clinical population sample and highlighted the role of the frontopolar cortex. Despite the growing interest in non-invasive brain stimulation technologies for addiction treatment, the ideal location for intervention is still elusive. Much of the initial attention in this field was focused on the DLPFC (88% of total tES trials) with more promising results with symmetric compared to asymmetric montages [29]. The importance of frontopolar areas was also reported in previous dose-response relationship research for people with SUDs. Esmaeilpour et al used atlas-based parcellation for defining ROIs over the head models and fMRI data during a standard

drug cue reactivity task were collected immediately before and after stimulation in a group of participants with MUDs. Their results showed a significant correlation between changes in brain activation and averaged EF strength only in the frontopolar cortex as the area that received maximum EF compared to other predefined regions [46]. Similar results were also found in a larger cohort of participants with MUDs; a significant correlation between the normal component of the EF and changes in functional activity in the frontopolar cortex was reported during a drug cue reactivity task.

Our suggestion about the importance of frontopolar areas in tES for addiction conforms with recent evidence obtained from lesion-based studies that reported the frontopolar cortex as a key region in trans-diagnostically relevant neural circuits contributing to addiction [76]. Lesion-based fMRI data revealed that a higher likelihood of decreasing substance use was associated with brain injury to areas that had negative connectivity to the frontopolar areas and recommended frontopolar as an ideal neuromodulation treatment target for addiction in future studies [76]. In addition to within-group variability, our between-group results suggest that EF distribution patterns cannot be simply transferred from healthy to clinical populations and more research is still needed to pinpoint the optimal target, stimulation dose over the targeted region, and ultimately maximize clinical benefits at individual/group-levels.

4.10. Limitations and future directions

Our study has some limitations that could be addressed in future research. The main limitation is that we only focused on the structural MRI and simulation approaches. We did not consider other behavioral/neural outcomes to determine the role of EFs in each targeted and non-targeted brain region. Our findings are specific to stimulation alone. The context of the received dose over the cortex also guides the induced neuroplasticity (e.g., if stimulation is delivered while participants are performing a specific cognitive task, the engaged brain regions for task performance will also experience plasticity). Furthermore, in our clinical population, we did not examine the relationship between EFs and clinical response (e.g., drug consumption/craving). Open questions remain about how to relate EFs with behavioral or neurophysiological changes in both healthy and clinical populations. The relationship between EF peaks and stimulation outcomes is not a trivial matter and there is still no clear understanding of the underlying neural substrates. More neuroimaging/neurophysiological assessments are needed to determine the causal role of medial frontopolar cortices in response to bipolar DLPFC stimulation. Furthermore, since we did not consider age/sex-matched clinical population and because the imaging protocols were different between the two groups, we did not directly compare our results between MUDs and healthy subjects as conducted by [47]. Because it has been reported that EF distribution patterns in brain stimulation studies may be different in the field of addiction compared to healthy subjects with respect to the brain anatomical alterations [65, 66] and because sex differences in skull thickness, for example, would lead to differences in peak EF location/value, comparing EF peaks between SUDs and healthy subjects in age and sex-matched case-control cohorts could be further investigated in future studies. For instance, our results showed that the center of averaged EF peak location is deeper in the brain of our clinical population compared to healthy subjects. The main reason could be investigated in future studies.

5. Conclusion

Here, we discussed that, in two of the most frequently used electrode montages in tES studies which are commonly intended for modulating DLPFC, DLPFC was not maximally targeted by placing large electrodes over this region and other parts of the prefrontal cortex also received strong electric field strength.

Considering inter-individual variability, our results highlighted the crucial role of the frontopolar area in tES over DLPFC. Based on individual and group-level analysis of EF peaks, in both healthy subjects and MUDs, we recommend avoiding attributing F3/F4 tES results (with symmetric or asymmetric configuration) only to DLPFC. Other brain regions in medial prefrontal areas like medial frontopolar should be considered in upcoming trials placing large electrode pads over DLPFC.

Supplementary materials:

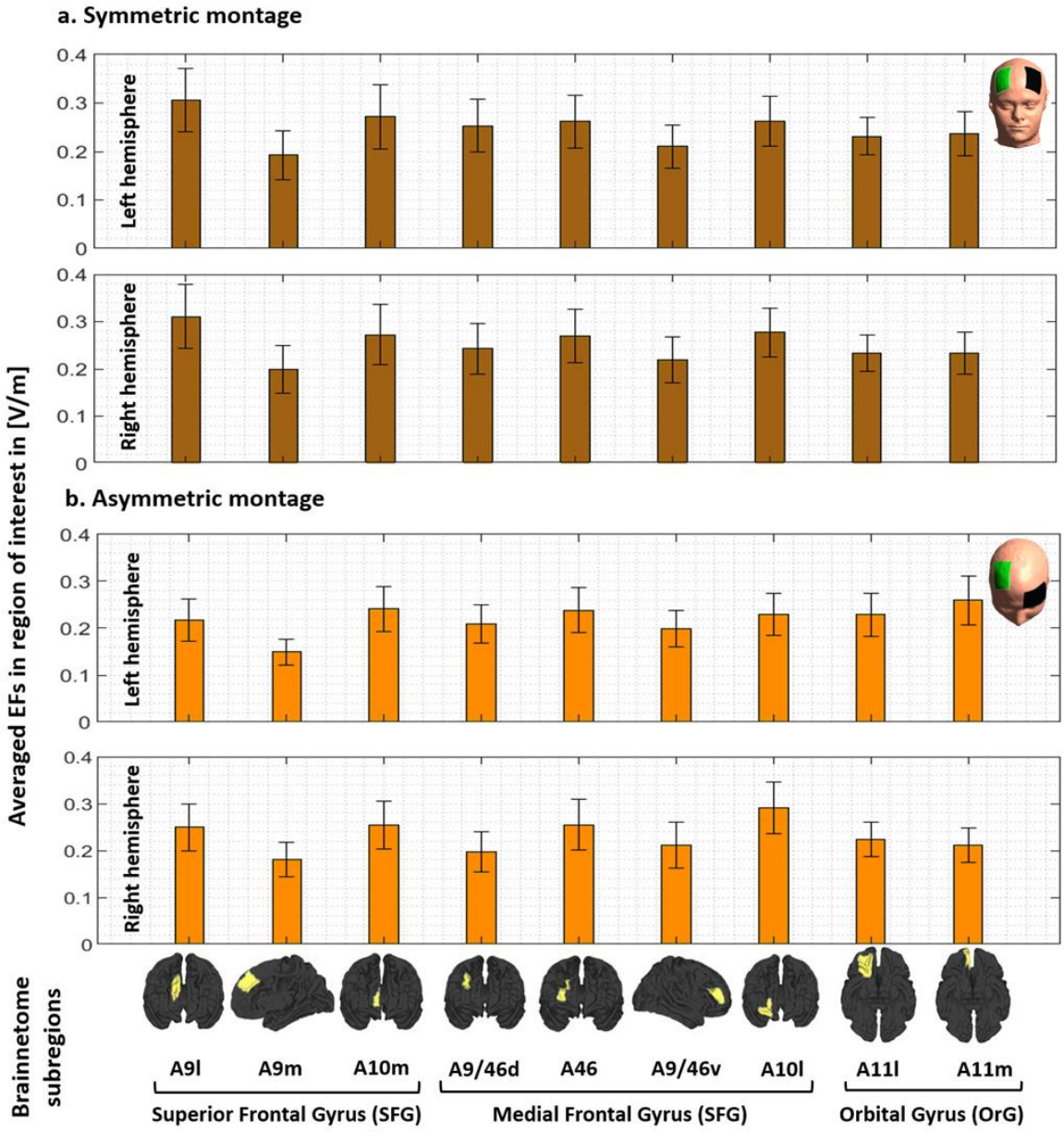

Figure S1. EF strength within the main subregions of the prefrontal cortex. Computational head models were generated for all participants and a Brainnetome atlas with 105 subregions in each hemisphere was used to extract tES-induced EFs in each cortical areas based on **(a)** symmetric (dark brown) and **(b)** asymmetric (light brown) montages. Bars show mean values and error bars show standard deviations (SD) of the EF strength in volt per meter ([V/m]) across 77 healthy subjects in 9 main subregions of the prefrontal cortex in the left (lines 1 and 3) and right (line 2 and 4) hemispheres. Labels below the horizontal axis determine the name of each subregion based on Brainnetome atlas parcellations and small brains next to the labels represent each region in fsaverage space. Atlas-based parcellation: *Superior frontal gyrus:* A9l, lateral area [13,48,40], A9m, medial area [6,38,35], A10m: medial area [8,58,13]. *Middle frontal gyrus:* A9/46d, dorsal area [30,37,36], A9/46v, ventral area [42,44,14], A46 [28,55,17], A10l, lateral area [25,61,-4]. *Orbital gyrus*: A11l, lateral area [23,36,-18], and A11m, medial area [6,57,-16]. Abbreviation: EF: electric field, SFG: superior frontal gyrus, MFG: medial frontal gyrus, OrG: orbital gurus.

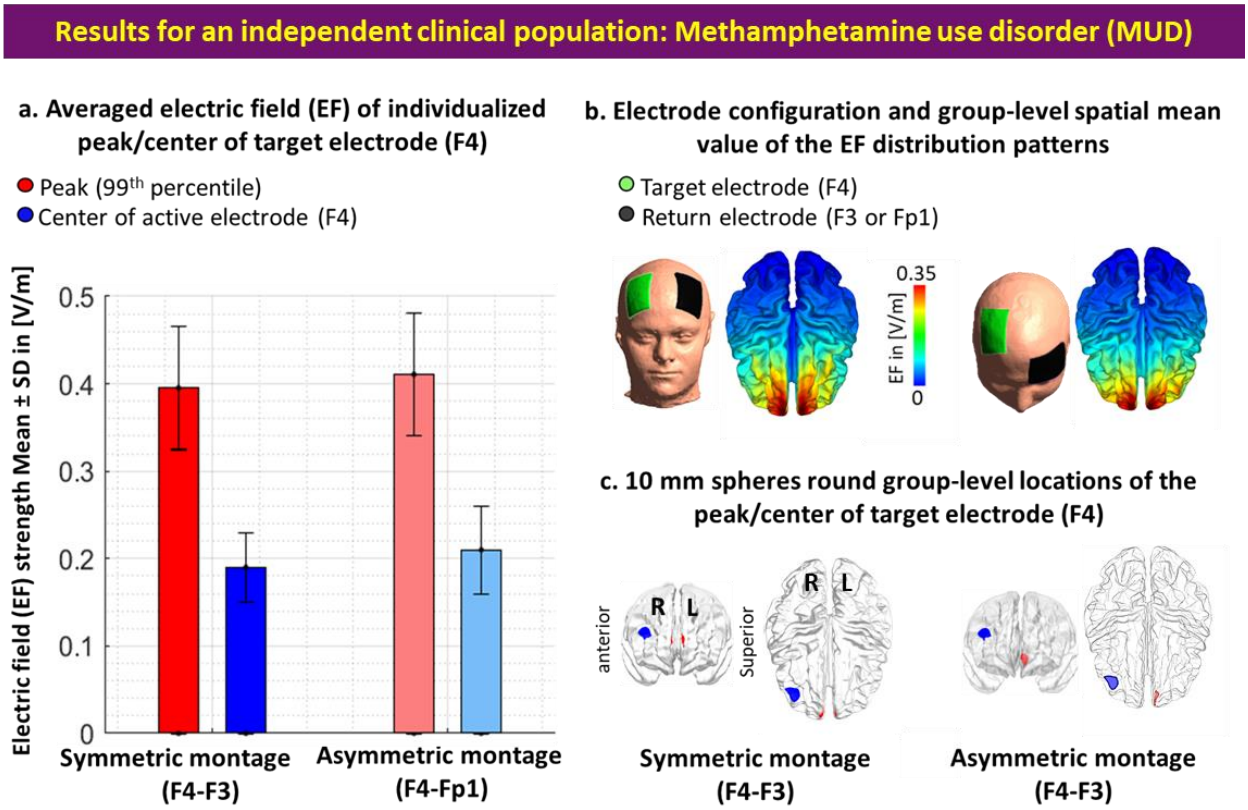

Figure S2. Comparing the center of the target electrode with EF peaks in an independent clinical population-people with methamphetamine use disorder (MUD). a. Bars show mean values and error bars show standard deviations (SD) of the EF strength in volt per meter ([V/m]) across 66 participants with MUD in individualized 99th percentile of the EF (peaks, in red) and center of the target electrode (F4, in blue) over the cortex across the population for symmetric (target/return over F4/F3 in dark colors) and asymmetric (target/return over F4/Fp1 in light colors) montages. Target electrodes over F4 are depicted in green, return electrodes over F3 in symmetric, and Fp1 in asymmetric montages are depicted in black. **b.** Electrode configurations over the scalp for DLPFC stimulation are visualized with the target (in green)/return (in black) electrodes over F4/F3 in symmetric and F4/Fp1 in asymmetric montages. EF distribution patterns at the group-level (spatial mean values across the population) are visualized over the cortex in superior view. **c.** Locations of the 10 mm spheres around F4 (in blue) and averaged location of the peaks across the population (in red) are visualized over the standard brain in fsaverage space. In each panel, the left side corresponds to symmetric montage (F4-F3) and right side corresponds to asymmetric (F4-Fp1) montages. Abbreviation: EF: electric field.

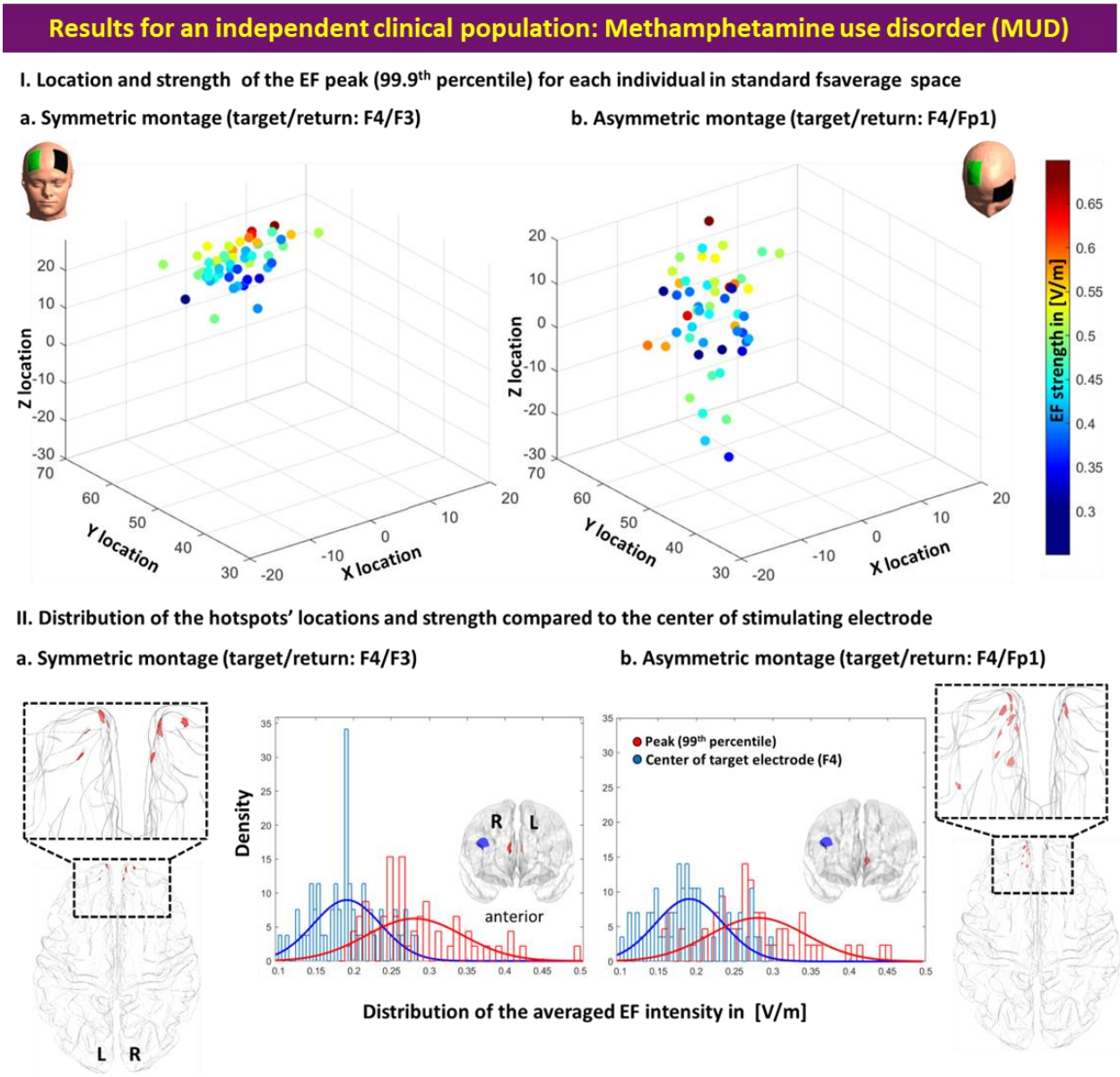

Figure S3. Inter-individual variability of peak EF location and strength in an independent clinical population-people with methamphetamine use disorder (MUD). I. Scatter plot (for location in MNI space) colored based on EF strength (hot colors represent strong EF strength) for visualizing inter-individual variability in the 99th percentile of the EFs in symmetric **(a)** and asymmetric **(b)** DLPFC montages. **II.** Visualizing the location of the 99th percentile of the EF over the standard fsaverage space (red dots over the cortex represent each individual). Distribution plots represent the distribution of the EF strength within the 10 mm spheres around F4 and 99th percentile (blue and red spheres over the cortex in anterior view) for symmetric **(a)** and asymmetric **(b)** montages. Abbreviation: EF: electric field.

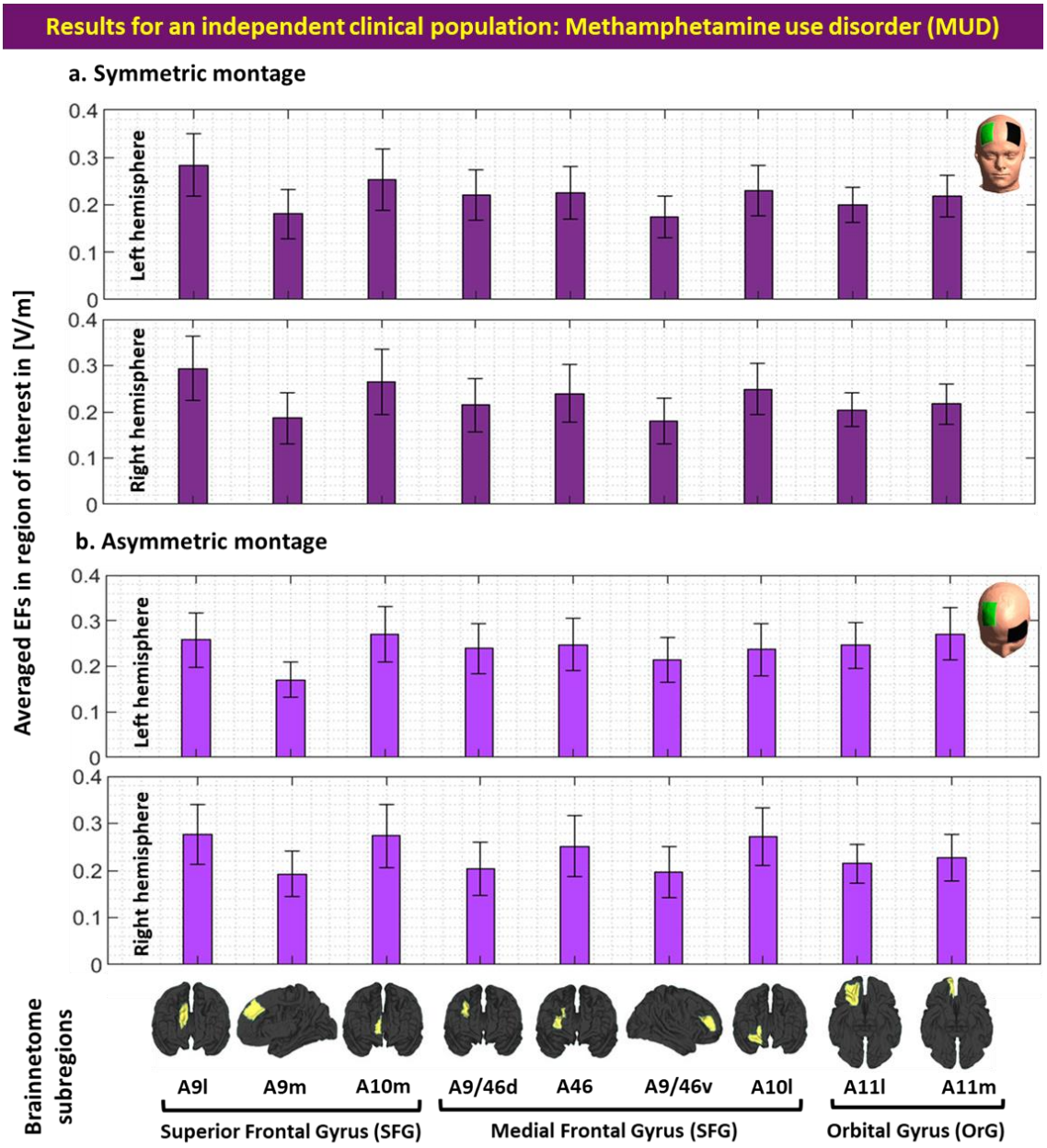

Figure S4. EF strength within the main subregions of the prefrontal cortex in an independent clinical population-people with methamphetamine use disorder (MUD). Computational head models were generated for all participants and a Brainnetome atlas with 105 subregions in each hemisphere was used to extract tES-induced EFs in each cortical areas based on **(a)** symmetric (dark green) and **(b)** asymmetric (light green) montages. Bars show mean values and error bars show standard deviations (SD) of the EF strength in volt per meter ([V/m]) across 66 participants with methamphetamine use disorder (MUD) in 9 main subregions of the prefrontal cortex in the left (line 1 and 3) and right (line 2 and 4) hemispheres. Labels below the horizontal axis determine the name of each subregion based on Brainnetome atlas parcellations and small brains next to the labels represent each region in fsaverage space. Atlas-based parcellation: *Superior frontal gyrus:* A9l, lateral area [13,48,40], A9m, medial area [6,38,35], A10m: medial area [8,58,13]. *Middle frontal gyrus:* A9/46d, dorsal area [30,37,36], A9/46v, ventral area [42,44,14], A46 [28,55,17], A10l, lateral area [25,61,-4]. *Orbital gyrus*: A11l, lateral area [23,36,-18], and A11m, medial area [6,57,-16]. Abbreviation: EF: electric field, SFG: superior frontal gyrus, MFG: medial frontal gyrus, OrG: orbital gurus.

References

1. Duncan, J. and A.M. Owen, *Dissociative methods in the study of frontal lobe function.* Attention and Performance, 2000. **18**: p. 566-576.
2. Hoshi, E., *Functional specialization within the dorsolateral prefrontal cortex: a review of anatomical and physiological studies of non-human primates.* Neuroscience research, 2006. **54**(2): p. 73-84.
3. Grimm, S., et al., *Imbalance between left and right dorsolateral prefrontal cortex in major depression is linked to negative emotional judgment: an fMRI study in severe major depressive disorder.* Biological psychiatry, 2008. **63**(4): p. 369-376.
4. Smucny, J., et al., *Mechanisms underlying dorsolateral prefrontal cortex contributions to cognitive dysfunction in schizophrenia.* Neuropsychopharmacology, 2022. **47**(1): p. 292-308.
5. Goldstein, R.Z. and N.D. Volkow, *Dysfunction of the prefrontal cortex in addiction: neuroimaging findings and clinical implications.* Nature reviews neuroscience, 2011. **12**(11): p. 652-669.
6. Dedoncker, J., et al., *A systematic review and meta-analysis of the effects of transcranial direct current stimulation (tDCS) over the dorsolateral prefrontal cortex in healthy and neuropsychiatric samples: influence of stimulation parameters.* Brain stimulation, 2016. **9**(4): p. 501-517.
7. Naish, K.R., et al., *Effects of neuromodulation on cognitive performance in individuals exhibiting addictive behaviors: a systematic review.* Drug and alcohol dependence, 2018. **192**: p. 338-351.
8. Kim, W.-J., et al., *Neuronavigation-guided repetitive transcranial magnetic stimulation for aphasia.* JoVE (Journal of Visualized Experiments), 2016(111): p. e53345.
9. Modak, A. and P.B. Fitzgerald, *Personalising transcranial magnetic stimulation for depression using neuroimaging: a systematic review.* The World Journal of Biological Psychiatry, 2021. **22**(9): p. 647-669.
10. Rusjan, P.M., et al., *Optimal transcranial magnetic stimulation coil placement for targeting the dorsolateral prefrontal cortex using novel magnetic resonance image-guided neuronavigation*. 2010, Wiley Online Library.
11. Soleimani, G., et al., *How structural and functional MRI can inform dual-site tACS parameters: A case study in a clinical population and its pragmatic implications.* Brain stimulation, 2022.
12. Jasper, H.H., *The ten-twenty electrode system of the International Federation.* Electroencephalogr. Clin. Neurophysiol., 1958. **10**: p. 370-375.
13. Woods, A.J., et al., *A technical guide to tDCS, and related non-invasive brain stimulation tools.* Clinical Neurophysiology, 2016. **127**(2): p. 1031-1048.
14. Herwig, U., P. Satrapi, and C. Schönfeldt-Lecuona, *Using the international 10-20 EEG system for positioning of transcranial magnetic stimulation.* Brain topography, 2003. **16**(2): p. 95-99.
15. Datta, A., et al., *Gyri-precise head model of transcranial direct current stimulation: improved spatial focality using a ring electrode versus conventional rectangular pad.* Brain stimulation, 2009. **2**(4): p. 201-207. e1.
16. Miranda, P.C., P. Faria, and M. Hallett, *What does the ratio of injected current to electrode area tell us about current density in the brain during tDCS?* Clinical Neurophysiology, 2009. **120**(6): p. 1183-1187.
17. Opitz, A., et al., *Determinants of the electric field during transcranial direct current stimulation.* Neuroimage, 2015. **109**: p. 140-150.
18. Edwards, D., et al., *Physiological and modeling evidence for focal transcranial electrical brain stimulation in humans: a basis for high-definition tDCS.* Neuroimage, 2013. **74**: p. 266-275.
19. Brunoni, A.R., et al., *The sertraline vs electrical current therapy for treating depression clinical study: results from a factorial, randomized, controlled trial.* JAMA psychiatry, 2013. **70**(4): p. 383-391.

20. Ironside, M., et al., *Frontal cortex stimulation reduces vigilance to threat: implications for the treatment of depression and anxiety.* Biological psychiatry, 2016. **79**(10): p. 823-830.
21. Csifcsák, G., et al., *Effects of transcranial direct current stimulation for treating depression: A modeling study.* Journal of affective disorders, 2018. **234**: p. 164-173.
22. Juckel, G., A. Mendlin, and B.L. Jacobs, *Electrical stimulation of rat medial prefrontal cortex enhances forebrain serotonin output: implications for electroconvulsive therapy and transcranial magnetic stimulation in depression.* Neuropsychopharmacology, 1999. **21**(3): p. 391-398.
23. Diederichs, C., et al., *Intermittent theta-burst stimulation transcranial magnetic stimulation Increases GABA in the medial prefrontal cortex: a preliminary sham-controlled magnetic resonance spectroscopy study in acute bipolar depression.* Frontiers in psychiatry, 2021. **12**: p. 649.
24. Callejón-Leblic, M. and P.C. Miranda, *A computational parcellated brain model for electric field analysis in transcranial direct current stimulation.* Brain Hum Body Model, 2020. **2020**: p. 81.
25. Soleimani, G., et al., *Group and individual level variations between symmetric and asymmetric DLPFC montages for tDCS over large scale brain network nodes.* Scientific Reports, 2021. **11**(1): p. 1271.
26. Li, L.M., K. Uehara, and T. Hanakawa, *The contribution of interindividual factors to variability of response in transcranial direct current stimulation studies.* Frontiers in cellular neuroscience, 2015. **9**: p. 181.
27. Vergallito, A., et al., *Inter-Individual Variability in tDCS Effects: A Narrative Review on the Contribution of Stable, Variable, and Contextual Factors.* Brain Sciences, 2022. **12**(5): p. 522.
28. Thielscher, A., A. Antunes, and G.B. Saturnino. *Field modeling for transcranial magnetic stimulation: a useful tool to understand the physiological effects of TMS?* in *2015 37th annual international conference of the IEEE engineering in medicine and biology society (EMBC)*. 2015. IEEE.
29. Ekhtiari, H., et al., *Transcranial electrical and magnetic stimulation (tES and TMS) for addiction medicine: A consensus paper on the present state of the science and the road ahead.* Neuroscience & Biobehavioral Reviews, 2019.
30. Fan, L., et al., *The human brainnetome atlas: a new brain atlas based on connectional architecture.* Cerebral cortex, 2016. **26**(8): p. 3508-3526.
31. Suen, P.J., et al., *Association between tDCS computational modeling and clinical outcomes in depression: data from the ELECT-TDCS trial.* European archives of psychiatry and clinical neuroscience, 2021. **271**(1): p. 101-110.
32. Rajkowska, G. and P.S. Goldman-Rakic, *Cytoarchitectonic definition of prefrontal areas in the normal human cortex: II. Variability in locations of areas 9 and 46 and relationship to the Talairach Coordinate System.* Cerebral cortex, 1995. **5**(4): p. 323-337.
33. Cardenas, V., et al., *Anatomical and fMRI-network comparison of multiple DLPFC targeting strategies for repetitive transcranial magnetic stimulation treatment of depression.* Brain stimulation, 2022. **15**(1): p. 63-72.
34. Khorrampanah, M., et al., *Optimization of montages and electric currents in tDCS.* Computers in Biology and Medicine, 2020. **125**: p. 103998.
35. Im, C.-H., et al., *Evaluation of local electric fields generated by transcranial direct current stimulation with an extracephalic reference electrode based on realistic 3D body modeling.* Physics in Medicine & Biology, 2012. **57**(8): p. 2137.
36. Kasten, F.H., et al., *Integrating electric field modeling and neuroimaging to explain inter-individual variability of tACS effects.* Nature communications, 2019. **10**(1): p. 1-11.
37. Huang, Y., et al., *Measurements and models of electric fields in the in vivo human brain during transcranial electric stimulation.* Elife, 2017. **6**: p. e18834.

38. Mikkonen, M., et al., *Cost of focality in TDCS: Interindividual variability in electric fields.* Brain stimulation, 2020. **13**(1): p. 117-124.
39. Caulfield, K.A. and M.S. George, *Optimizing transcranial direct current stimulation (tDCS) electrode position, size, and distance doubles the on-target cortical electric field: Evidence from 3000 Human Connectome Project models.* bioRxiv, 2021.
40. Hill, A.T., P.B. Fitzgerald, and K.E. Hoy, *Effects of anodal transcranial direct current stimulation on working memory: a systematic review and meta-analysis of findings from healthy and neuropsychiatric populations.* Brain stimulation, 2016. **9**(2): p. 197-208.
41. Horvath, J.C., J.D. Forte, and O. Carter, *Quantitative review finds no evidence of cognitive effects in healthy populations from single-session transcranial direct current stimulation (tDCS).* Brain stimulation, 2015. **8**(3): p. 535-550.
42. Wiethoff, S., M. Hamada, and J.C. Rothwell, *Variability in response to transcranial direct current stimulation of the motor cortex.* Brain stimulation, 2014. **7**(3): p. 468-475.
43. Laakso, I., et al., *Can electric fields explain inter-individual variability in transcranial direct current stimulation of the motor cortex?* Scientific reports, 2019. **9**(1): p. 1-10.
44. Laakso, I., et al., *Inter-subject variability in electric fields of motor cortical tDCS.* Brain stimulation, 2015. **8**(5): p. 906-913.
45. Gomez-Tames, J., et al., *Group-level and functional-region analysis of electric-field shape during cerebellar transcranial direct current stimulation with different electrode montages.* Journal of neural engineering, 2019. **16**(3): p. 036001.
46. Esmaeilpour, Z., et al., *Methodology for tDCS integration with fMRI.* Human brain mapping, 2020. **41**(7): p. 1950-1967.
47. Mizutani-Tiebel, Y., et al., *Differences in electric field strength between clinical and non-clinical populations induced by prefrontal tDCS: A cross-diagnostic, individual MRI-based modeling study.* NeuroImage: Clinical, 2022. **34**: p. 103011.
48. Schaefer, A., et al., *Local-global parcellation of the human cerebral cortex from intrinsic functional connectivity MRI.* Cerebral cortex, 2018. **28**(9): p. 3095-3114.
49. Green, A.E., et al., *Thinking cap plus thinking zap: tDCS of frontopolar cortex improves creative analogical reasoning and facilitates conscious augmentation of state creativity in verb generation.* Cerebral Cortex, 2017. **27**(4): p. 2628-2639.
50. Wang, J., et al., *Transcranial Direct Current Stimulation (tDCS) over the Frontopolar Cortex (FPC) Alters the Demand for Precommitment.* Behavioural Brain Research, 2021. **414**: p. 113487.
51. Riedel, P., et al., *Modulating functional connectivity between medial frontopolar cortex and amygdala by inhibitory and excitatory transcranial magnetic stimulation.* Human brain mapping, 2019. **40**(15): p. 4301-4315.
52. Fonzo, G.A., et al., *Selective effects of psychotherapy on frontopolar cortical function in PTSD.* American Journal of Psychiatry, 2017. **174**(12): p. 1175-1184.
53. Esmaeilpour, Z., et al., *Incomplete evidence that increasing current intensity of tDCS boosts outcomes.* Brain stimulation, 2018. **11**(2): p. 310-321.
54. Halko, M., et al., *Neuroplastic changes following rehabilitative training correlate with regional electrical field induced with tDCS.* Neuroimage, 2011. **57**(3): p. 885-891.
55. Lang, S., et al., *Preoperative transcranial direct current stimulation in glioma patients: a proof of concept pilot study.* Frontiers in neurology, 2020: p. 1518.
56. Antonenko, D., et al., *Towards precise brain stimulation: Is electric field simulation related to neuromodulation?* Brain stimulation, 2019. **12**(5): p. 1159-1168.
57. Jamil, A., et al., *Current intensity-and polarity-specific online and aftereffects of transcranial direct current stimulation: An fMRI study.* Human brain mapping, 2020. **41**(6): p. 1644-1666.

58. Indahlastari, A., et al., *Individualized tDCS modeling predicts functional connectivity changes within the working memory network in older adults.* Brain Stimulation, 2021. **14**(5): p. 1205-1215.
59. Kessler, S.K., et al., *Dosage considerations for transcranial direct current stimulation in children: a computational modeling study.* PloS one, 2013. **8**(9): p. e76112.
60. Faria, P., M. Hallett, and P.C. Miranda, *A finite element analysis of the effect of electrode area and inter-electrode distance on the spatial distribution of the current density in tDCS.* Journal of neural engineering, 2011. **8**(6): p. 066017.
61. Vöröslakos, M., et al., *Direct effects of transcranial electric stimulation on brain circuits in rats and humans.* Nature communications, 2018. **9**(1): p. 1-17.
62. Boggio, P.S., et al., *Modulation of risk-taking in marijuana users by transcranial direct current stimulation (tDCS) of the dorsolateral prefrontal cortex (DLPFC).* Drug and alcohol dependence, 2010. **112**(3): p. 220-225.
63. Fecteau, S., et al., *Modulation of smoking and decision-making behaviors with transcranial direct current stimulation in tobacco smokers: a preliminary study.* Drug and Alcohol Dependence, 2014. **140**: p. 78-84.
64. Weber, M.J., et al., *Prefrontal transcranial direct current stimulation alters activation and connectivity in cortical and subcortical reward systems: A tDCS-fMRI study.* Human brain mapping, 2014. **35**(8): p. 3673-3686.
65. McCalley, D.M. and C.A. Hanlon, *Regionally specific gray matter volume decreases in Alcohol Use Disorder: Implications for non-invasive brain stimulation treatment: Implications for non-invasive brain stimulation treatment.* Alcoholism: Clinical and Experimental Research, 2021.
66. Soleimani, G., et al., *Cortical Morphology in Cannabis Use Disorder: Implications for Transcranial Direct Current Stimulation Treatment.* Basic and Clinical Neuroscience: p. 0-0.
67. Parlikar, R., et al., *High definition transcranial direct current stimulation (HD-tDCS): A systematic review on the treatment of neuropsychiatric disorders.* Asian Journal of Psychiatry, 2021. **56**: p. 102542.
68. Cash, R.F., et al., *Functional magnetic resonance imaging–guided personalization of transcranial magnetic stimulation treatment for depression.* JAMA psychiatry, 2021. **78**(3): p. 337-339.
69. Oathes, D.J., et al., *Resting fMRI-guided TMS results in subcortical and brain network modulation indexed by interleaved TMS/fMRI.* Experimental brain research, 2021. **239**(4): p. 1165-1178.
70. Liston, C., *fMRI-guided methods for rTMS targeting and treatment prediction.* Brain Stimulation: Basic, Translational, and Clinical Research in Neuromodulation, 2021. **14**(6): p. 1737.
71. Ruffini, G., et al., *Optimization of multifocal transcranial current stimulation for weighted cortical pattern targeting from realistic modeling of electric fields.* Neuroimage, 2014. **89**: p. 216-225.
72. Fischer, D., et al., *Multifocal tDCS targeting the resting state motor network increases cortical excitability beyond traditional tDCS targeting unilateral motor cortex.* Neuroimage, 2017. **157**: p. 34-44.
73. Soleimani, G., et al., *Closing the loop between brain and electrical stimulation: Towards precision neuromodulation treatments.* 2022.
74. Chase, H.W., et al., *Transcranial direct current stimulation: a roadmap for research, from mechanism of action to clinical implementation.* Molecular psychiatry, 2020. **25**(2): p. 397-407.
75. Soleimani, G., et al., *DLPFC stimulation alters large-scale brain networks connectivity during a drug cue reactivity task: A tDCS-fMRI study.* Frontiers in systems neuroscience, 2022. **16**.
76. Joutsa, J., et al., *Brain lesions disrupting addiction map to a common human brain circuit.* Nature medicine, 2022: p. 1-7.